International Journal of Steel Structures 15(2): 299-310 (2015)
DOI 10.1007/s13296-014-1103-4

International Journal of
STEEL
STRUCTURES
www.springer.com/journal/13296

Investigations on the Effect of Weld Penetration on Fatigue Strength of Rib-to-Deck Welded Joints in Orthotropic Steel Decks

Cao Vu Dung[1,*], Eiichi Sasaki[1], Keiji Tajima[2], and Toshimitsu Suzuki[2]

[1]*Department of Civil Engineering, Tokyo Institute of Technology, 2-12-1 Ookayama, Meguro-ku, Tokyo, 152-8552, Japan*
[2]*Mitsubishi Heavy Industries Bridge & Steel Structures Engineering Co. Ltd, 5-1, Ebaokimachi, Naka-ku, Hiroshima, 730-8642, Japan*

Abstract

A common practice for the manufacture of orthotropic steel decks in Japan is to use 75% partial joint penetration welds between closed ribs and deck plates. To evaluate the effectiveness of the proposed 100% penetration on improving the fatigue strength of rib-to-deck welded joints in orthotropic steel bridge decks, four full-scale orthotropic deck specimens were subjected to laboratory testing. Specimens, consisting of a 12-mm-thick deck plate and 6-mm-thick rib, with one closed rib, were fabricated with 75% and 100% penetration. Fatigue test results showed that fatigue cracks initiated from the weld toe inside the rib in the 100% penetration specimens, but from weld root inside the rib in the 75% penetration specimens. To investigate this fatigue behavior, strain measurements were taken at 5 mm from the rib-to-deck weld line. Results of finite element analysis using the effective notch stress method indicate that a deeper partial penetration results in a slightly higher effective notch stress at the weld root of the partial penetration weld. The effective notch stress at the crack initiation location with 100% penetration is lower than that obtained with partial penetration. The open angle appears to have a significant effect on the effective notch stress at the upper weld toe when using 100% penetration. Therefore, the proposed 100% penetration appeared to have a positive effect on enhancing the fatigue resistance of rib-to-deck welded joints.

Keywords: fatigue, orthotropic deck, steel bridges, weld penetration, rib-to-deck joints, effective notch stress

1. Introduction

Orthotropic steel decks have been widely used for long and medium-sized bridges, including suspension bridges, cable-stay bridges, and urban elevated expressways due to their overall light weight, rapid erection, and structural redundancy. However, fatigue cracking has frequently been observed in rib-to-deck welded joints, due to high cyclic stresses and inadequate welding details (Bocchieri and Fisher, 1998). One-sided and Partial-Joint-Penetration (PJP) rib-to-deck welds are vulnerable to fatigue cracking due to a localized out-of-plane bending moment, particularly in the transverse direction, from the directly applied wheel loads (Miki, 2006).

In his excellent review of state-of-the-art fatigue strength assessment of welded structures, Radaj (1996) emphasized the significance of local design parameters in order to improve fatigue strength of the welded joints. In literature, a number of studies have focused on the effect of weld penetration which is defined as the ratio between the depth of penetration and the plate thickness.

Weld penetrations of 75% and 80% of the rib thickness are required by the Japan Road Association (JRA, 2002) and the AASHTO LRFD Bridge Design Specifications (AASHTO, 2010) respectively. Eighty percent penetration is more of a practical limit, i.e., the maximum penetration that could be achieved without regular Weld Melt-Through (WMT) (FWA, 2012).

Mori (2003) employed the four-point bending and pure tensile tests of rib-to-deck welded joints in which the rib was welded perpendicular to the deck plate and suggested that a deeper weld penetration (among 0, 25, 50, and 75% penetration ratios) tends to have a lower fatigue resistance. Meanwhile, Miki (2006) who used the finite element sub-models of the rib-to-deck joint derived from the global model of a real bridge reported that an increase in penetration (75% or less) results in lower effective notch stresses at the weld root, which results in higher fatigue resistance. A shallower weld penetration (for example, 80% PJP) appeared to have a slightly higher fatigue resistance than a deeper one (for example, 100% penetration with WMT) (Sim *et al*., 2009). Ya *et al*. (2011) conducted the vibration-based bending test with the specimens cut

Received January 31, 2014; accepted June 30, 2014;
published online December 12, 2014

*Corresponding author
Tel: +81-3-5734-3099; Fax: +81-3-5734-3577
E-mail: cao.v.ac@m.titech.ac.jp

from the original specimens tested by Sim *et al*. (2009) and concluded that WMT and 80% PJP details have comparable strength but that WMT has slightly lower fatigue strengths than the 80% PJP specimens. The finding is consistent with that of Sim *et al*. (2009). Finite-element analyses using effective notch stress method performed by Sim and Uang (2012) indicated that a shallower weld penetration (among 40%, 60%, and 80% penetration ratios) at the PJP joint has a positive effect in enhancing fatigue resistance.

Kusumoto *et al*. (2012) studied the effect of weld penetration on the fatigue behavior of the rib-to-deck weld joints by correlation between crack growth and variation of strain measured at 5 mm from the weld toe inside the rib and on top of the deck plate right above the weld during fatigue test. It was suggested that the strain variation pattern can help predict crack initiation and propagation for the 75 and 100% penetrations. Nishida *et al*. (2013) found that a two-sided fillet weld between the deck and the rib resulted in no significant improvement in fatigue strength compared to that of the conventional one-sided weld.

The literature review suggests that there has not been an agreement on the effect of weld penetration on fatigue resistance of rib-to-deck welded joints. In practice, it is difficult to consistently achieve the desired 75 and 80% without WMT or occasionally insufficient or excessive weld penetrations (i.e., penetration ratio lower or higher than 75 or 80%). So far the previous studies have focused on the effect of weld penetration which is lower than the design values. The effect of weld penetration higher than those values (75 or 80%) on fatigue strength of the rib-to-deck welded joints has not been well understood. (Sim and Uang, 2009) and (Ya *et al*., 2011) attempted to compare the fatigue strength of rib-to-deck welded joints with 80% penetration and WMT although the extent of WMT was not clearly defined since it was not controlled during manufacture of specimens. The uncertainty might add to the problem of scattering in weld geometry, and thus, in fatigue strength.

The authors hypothesized that if WMT is controlled by a weld penetration controlling device, consistency in weld penetration can be improved. Another advantage of the 100% penetration with controlled WMT is that fatigue crack initiates from the weld toe since there exists no weld root which is an inherent feature of the traditional partial penetration. The question then becomes whether the 100% penetration with controlled weld melt-through can improve the fatigue strength of the rib-to-deck welded joints of orthotropic steel bridge decks.

The objective of this research is to evaluate the effectiveness of the proposed 100% weld penetration on improving the fatigue resistance of rib-to-deck PJP welds. Fatigue testing was conducted on orthotropic deck specimens fabricated with two degrees of weld penetration, namely 75%, which is required by JRA (2002), and the proposed 100%, which is obtained by using WMT controlling techniques in fabrication (Fig. 1). Finite element method, using effective notch stress approach, was then employed to evaluate the local stress at crack initiation locations identified after the fatigue test to verify any improvement in stress condition for 100% penetration. The effect of weld penetration higher than 75% on the local effective notch stress was investigated in a parametric study.

2. Fatigue Testing Program

2.1. Specimen fabrication

Four specimens were fabricated by a commercial fabricator. SM400A steel was used for the specimens. Each specimen consisted of a 12-mm-thick deck plate and 6-mm-thick rib. The first and second specimens (abbreviated as S1 and S2, respectively) were fabricated with the proposed 100% penetration while the third and fourth specimens (S3 and S4, respectively) were created with the traditional 75% penetration (Table 1). To manufacture these experimental specimens, welding between a 1 m × 1.5 m steel deck plate and U-rib was conducted first by using a welding robot arm (Fig. 2). Four 30 cm-long portions were then cut from the post-weld rib-to-deck panel for further welding to the transverse girders, longitudinal girders and the lower flange. The size of each specimen was 100 cm × 30 cm (Fig. 4).

In order to achieve the desired 100% penetration, a weld penetration controlling equipment was installed inside the rib during the welding process. Weld penetration was controlled by a backing bar that was positioned at the rib-to-deck joint inside the closed rib during welding. A slope of 1:2 was beveled so that the weld bead inside the rib would be shaped in the configuration shown in Fig.

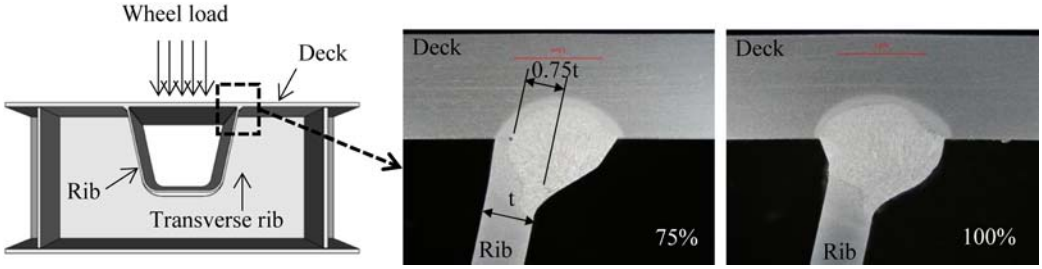

Figure 1. Rib-to-deck welded joints fabricated with 75% and 100% penetration.

Table 1. Configuration of the welded joints illustrated in Fig. 3

	100% penetration				75% penetration			
	S1		S2		S3		S4	
	①	②	①	②	①	②	①	②
a (mm)	9.7	9.1	9.9	8.6	9.6	8.9	8.8	9.0
b (mm)	6.7	6.1	5.3	6.8	7.5	6.7	8.3	6.7
c (mm)	2.9	4.1	5.7	3.2	2.0	3.7	1.6	1.8
d (mm)	1.6	2.1	3.1	0.9		1.1*		
θ_1 (^{0})	84	83	84	81	55	60	55	56
θ_2 (^{0})	74.5	72	68	104		110		

①② : The 1st and 2nd weld lines of each specimen (S1-S4)
* Weld melt-through was observed in a small portion of the weld line.

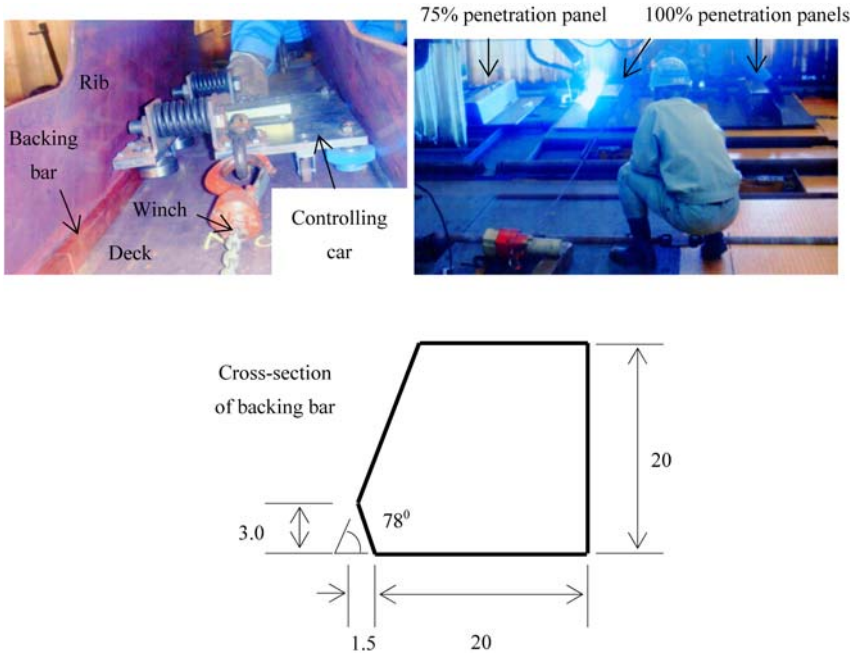

Figure 2. Application of backing bar for controlling weld penetration during fabrication of 100% penetration rib-to-deck welded joints.

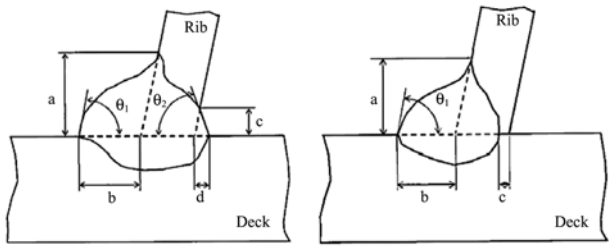

(a) 100% Penetration (b) 75% Penetration

Figure 3. Weld configuration.

3a. The cross section of the backing bar that was made from copper is shown in Fig. 2. The backing bar was kept in position by two springs attached on the controlling car. The movement of the controlling car in the longitudinal direction was tuned by pulling the winch to match the movement of the welding torch that was carried by the robot arm outside the rib during welding. The force of the two springs was kept minimal so that longitudinal movement was not impeded due to friction. This welding method was not employed in the welding procedure for 75% penetration.

2.2. Test setup and loading scheme

Figure 4 shows the plan, elevation, and cross-sectional views of the test specimens. In S1 and S2, nine strain gages were located under the deck plate along the weld line, at a distance of 5 mm from the weld toe inside the rib (Fig. 6). However, in S3 and S4, nine gages were positioned at a distance of 5 mm from the edge of the rib plate. Strain measurement was simultaneously conducted at two opposite sides of the loading pad, along weld lines at the west side (W) and the east side (E). Definition of

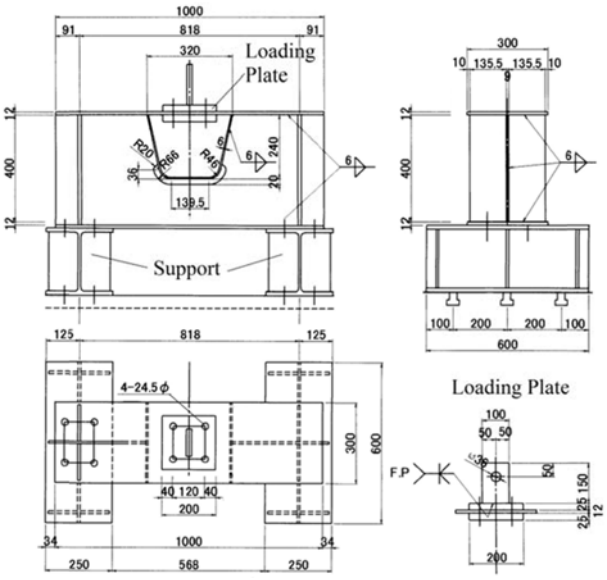

Figure 4. Specimen configuration (Unit: mm).

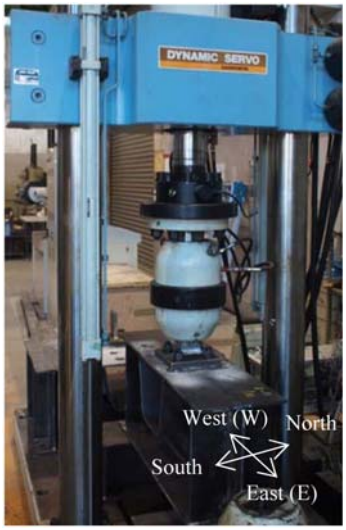

Figure 5. Test setup.

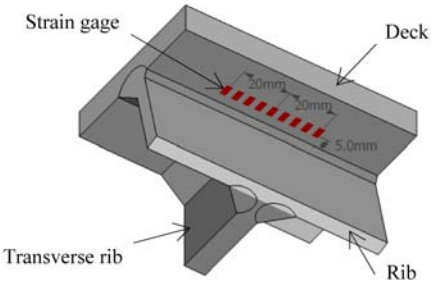

Figure 6. Location of strain gages.

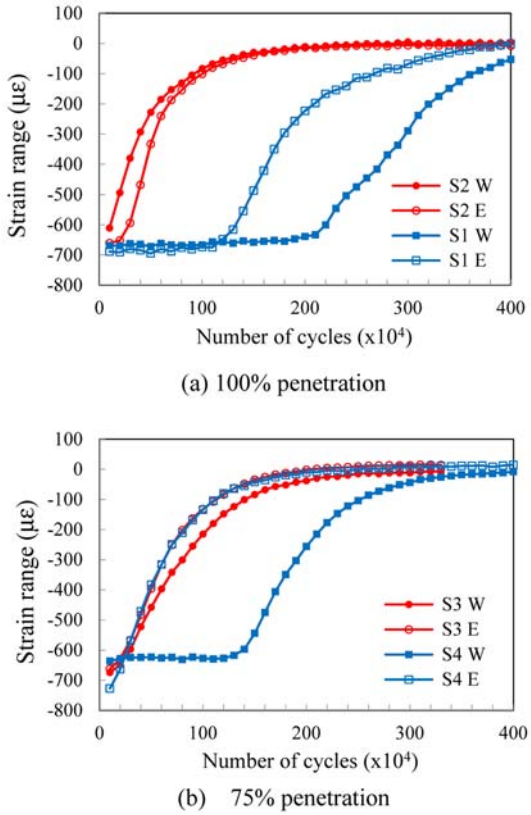

Figure 7. Comparison of strain range variation recorded by the strain gage where the first 20% strain range drop was observed.

the four cardinal directions is shown in the test setup (Fig. 5) with an actuator centered on top of the deck plate of the specimen. The specimen was supported by two supporting diaphragms like a simple beam. The applied load from the actuator simulated a single truck wheel load of 50 kN, which is half of the design axle load of 100 kN required by JRA (2002). The size of the loading pad was 20 cm × 20 cm. The initial loading ranged from -5 kN to -55 kN, then +5 kN to -45 kN after a 50% strain range drop had been observed at all strain gages located in the same weld line.

3. Experimental results

Fig. 7 shows the variation in strain range which is defined as the difference between strain recorded at −5 kN and -55 kN (or +5 kN and -45 kN after the load range was shifted) at the gage channel where the first 20% strain range drop was observed. S1 appeared to experience the first 50% strain range drop at both sides later than that of the remaining specimens (Fig. 8). This may indicate that S1 has the highest fatigue strength among all specimens. However, there was a large difference between the rate of strain range drop measured at S1 and S2. The difference suggests that S2 has significantly lower fatigue strength than S1. Meanwhile, S3 and S4 appeared to have comparable fatigue strengths except for the east side of S4 (Fig. 8).

In order to determine the cause of the large variation in fatigue strength of the 100% penetration specimens,

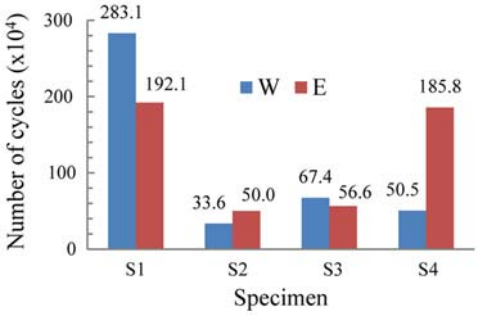

Figure 8. Number of cycles at the first 50% strain range drop.

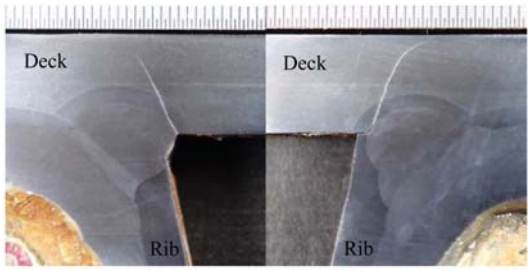

(a) 100% penetration (S1&S2) (b) 75% penetration (S3&S4)

Figure 9. Crack propagation pattern.

experimental specimens S1, S2, and S4 were cut perpendicular to the rib-to-deck weld line through the gage channel where the first 20% strain range drop was observed. Etching was performed on the section surfaces until the crack propagation pattern and weld profile could be visually observed (Fig. 9). In S1 and S2, fatigue cracks appeared to initiate from the weld toe inside the rib, unlike from the weld root in S3 and S4. All cracks propagated through the deck thickness but did not reach the deck surface (Fig. 9).

The etched surface in S2 (Fig. 10) reveals the existence of cold lap, a type of weld defect which occurs when molten metal does not completely fuse with the cold plate (base metal). Cold lap produces a crack-like defect, which has been reported to have a detrimental effect on fatigue strength of welded joints (Heiskanen, 2008). Cold lap can be visually seen in the west side of S2 and to a lesser extent in the east side of S2. However, cold lap does not exist at both sides of S1. Therefore, cold lap may be the cause of the lower fatigue strength of S2 compared to that of S1.

In an attempt to visually identify fatigue cracks, Magnetic Particle Testing (MT) was conducted. Fig. 11 shows the actual fatigue crack identified by MT at the weld toe inside the rib at the east side of S1. It was observed that the crack length had reached about 31 mm after 1.75 million cycles of loading. After 1.75 million cycles, the strain range drop recorded at the strain gage where the first 20% strain range drop was recorded, was 56% (Fig 7). This observation suggests that the crack initiated at a smaller number of cycles. In this study, the number of cycles at 20% strain range drop, which is for example 1.371 million cycles for the east side of S1, is defined as the initiation life of the rib-to-deck welded joint.

The variation of strain range drop after a certain number of cycles along the weld line suggests that fatigue crack may have initiated at the north side, at about 10 mm from the midpoint of the weld line, and then propagated towards

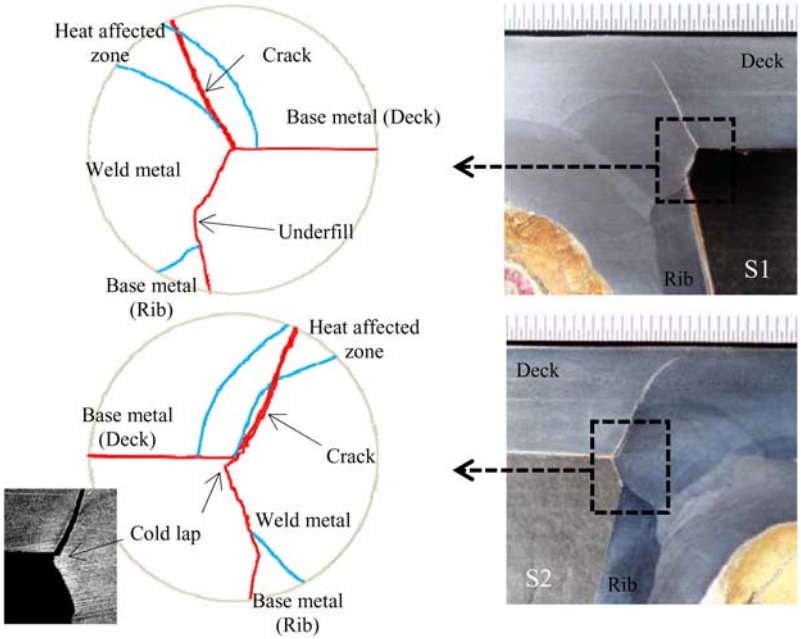

Figure 10. Etched surfaces of S1 and S2 showing weld configuration and existence of cold lap in S2.

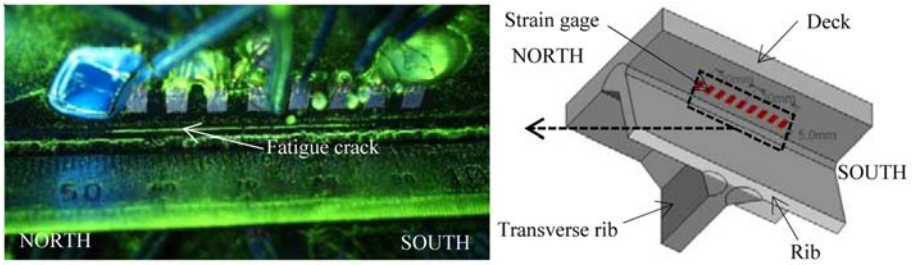

Figure 11. Fatigue crack at weld toe inside rib identified by magnetic particle testing performed at 1.75 million cycles at the east side of specimen S1.

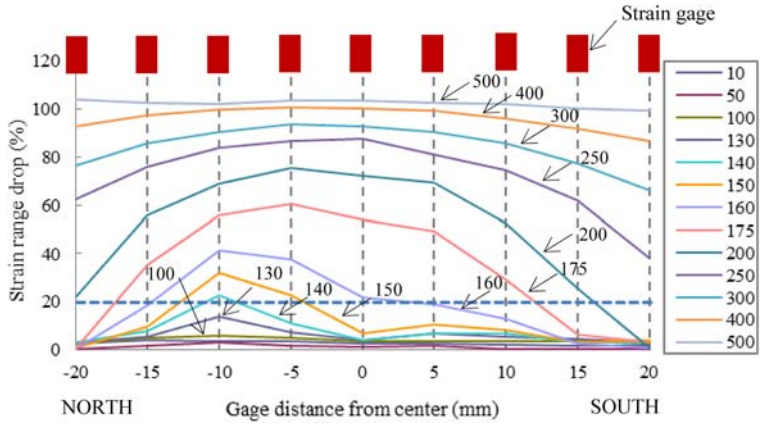

Figure 12. Variation of strain range drop recorded at the nine gages shown in Figure 11 at the east side of S1 (The legend shows the number of cycles [$\times 10^4$]).

the opposite side until a symmetric variation in strain range drop was observed (Fig. 12). Furthermore, the strain range drop variation curve between -15 mm and 15 mm, at 1.75 million cycles, appeared to agree with the crack location and length observed in the MT test (Fig. 12). This agreement was also observed in the application of strain range variation at 5 mm from weld toes to predict fatigue crack growth reported in literature (e.g., Kusumoto *et al*. (2012)).

4. Finite Element Analysis

4.1. Effect of cold lap

In an attempt to evaluate the effect of cold lap existence on the fatigue performance of the tested specimens, a two-dimensional (2D) solid elastic-plastic finite element analysis was conducted. Local plastic strain at the weld toe was evaluated through two scenarios; weld toe with and without cold lap.

A finite element model (Fig. 13) using 2D plane-strain solid elements was created to simulate the plane strain condition at the center of the tested specimens. The loading condition represents the maximum load of 55kN, which was applied on the deck plate of the tested specimens during experiment. Four-node elements (QUAD4) of 0.001 mm size were created at the notch. The gap induced by the cold lap defect was assumed to be 0.01 mm. The depth of the cold lap was 0.29 mm according to observation on the etched surface of the S2 specimen.

Both elastic and plastic constitutive models were defined. An elastic modulus of 200 GPa and a Poisson's ratio of 0.3 were assigned to the elastic properties. The Mises/Hill yield criteria and the isotropic hardening rule were chosen for the plastic properties. The true stress and plastic strain relationship obtained from the tensile test of the material used in the tested specimens was used as the input for the plastic constitutive model (Fig. 14).

As shown in Fig. 15, the maximum principal plastic strain with cold lap appeared to be 2.17 times of that obtained without cold lap. It is therefore reasonable to attribute the existence of cold lap as a possible cause of the deteriorated fatigue strength of rib-to-deck weld in the second specimen (S2) where cold lap existed.

4.2. Effect of weld penetration

To support the testing of the orthotropic deck specimens and to provide an additional insight into the fatigue behavior, a three-dimensional (3D) finite-element analysis of the experimental specimens was conducted to investigate the local stress at the crack initiation locations identified in fatigue testing. The effective notch stress method was employed to evaluate the stresses at the weld toe and the weld root of the rib-to-deck welded joints to verify the effectiveness of the proposed weld penetration on improving

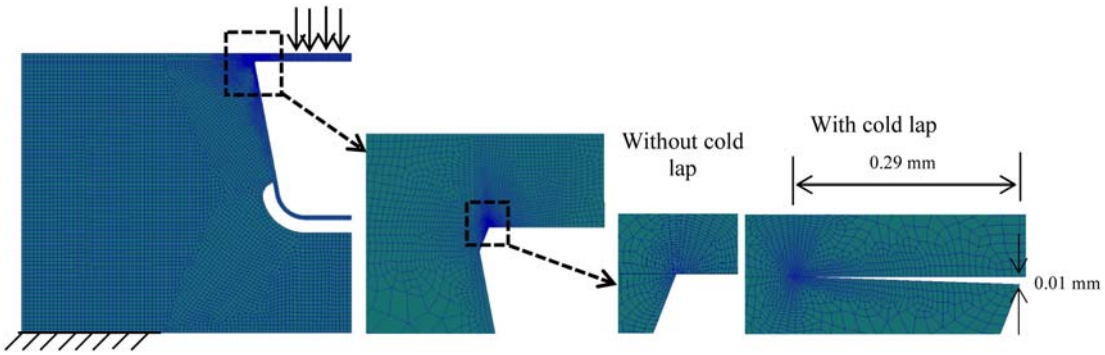

Figure 13. 2D finite element model of the 100% penetration created with and without cold lap existence at the upper weld toe.

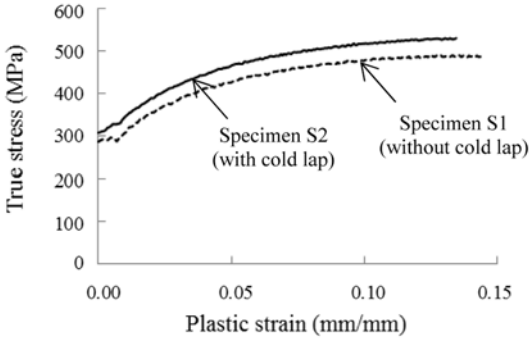

Figure 14. True stress - plastic strain relationship obtained from material tests.

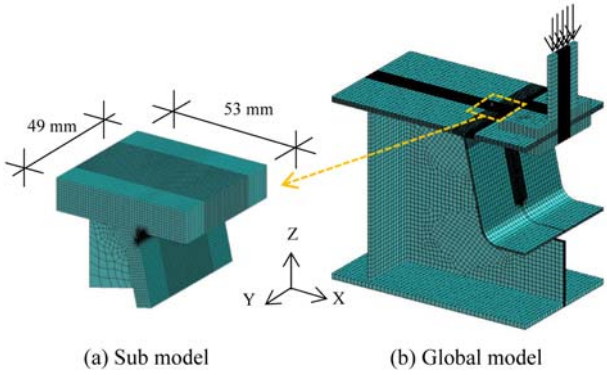

Figure 16. Finite-element models.

stress conditions. In addition, the effect of weld penetration ratio on fatigue resistance of rib-to-deck joints was evaluated in a parametric study.

Effective notch stress is defined as the total stress (for example, von Mises stress) at a notch assuming linear-elastic material behavior (Hobbacher, 2009). To take into account the variation of weld shape parameters and the non-linear material behavior at the notch root, the actual weld contour is replaced by an effective one (Hobbacher, 2009). The sub-modeling technique was used to model the tested specimens to obtain the local effective notch stresses. In the global model, 3D solid elements including TET4, WEDGE6, and HEX8, which have four, six, and eight nodes, respectively, were used due to the complexity of the rib-deck-girder joint geometry (Fig. 16). In particular, HEX8 elements with size of 1 mm were used at the locations where strain values would be compared to those obtained in the initial static test prior to the fatigue testing. To utilize symmetry, half of the specimen was modeled. A Young's modulus of 200 GPa and a Poisson's ratio of 0.3 were assigned to the elastic material properties. The area of the specimen's lower flange resting on the support diaphragms were restrained in all directions and all nodes on the symmetric plane were restrained in the transverse (x-direction) and not allowed to rotate about the longitudinal (y-axis) (Fig. 16).

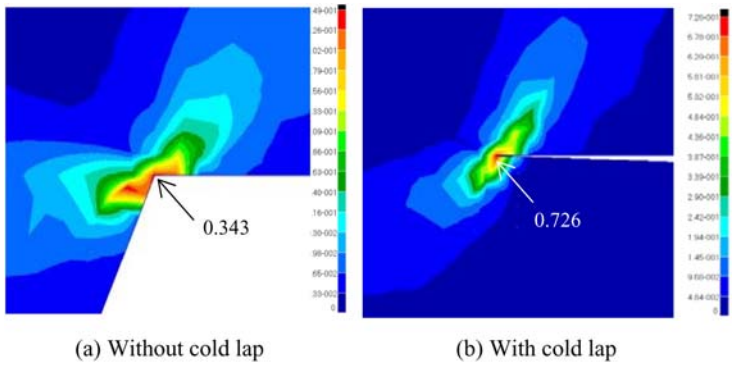

Figure 15. Distribution of maximum principal strain at notch.

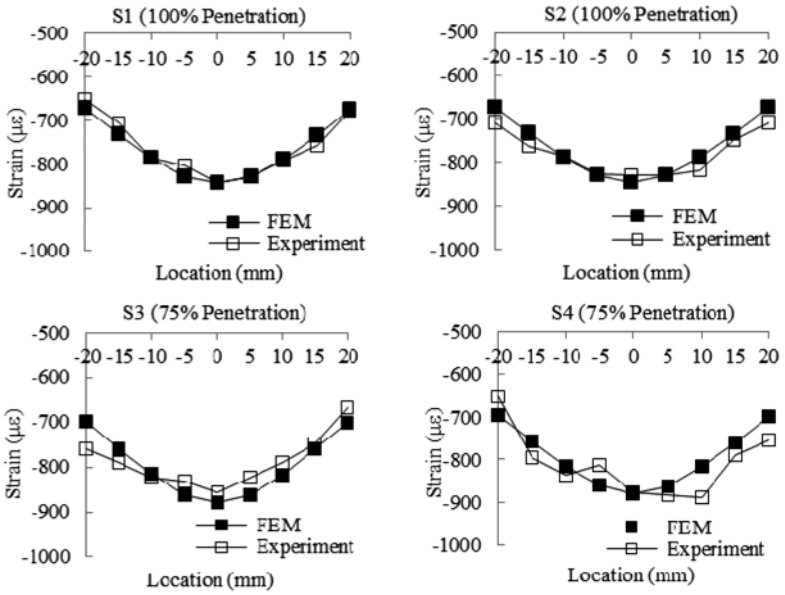

Figure 17. Comparison of strain values obtained by FE analysis and those recorded in the initial static test conducted during experiment.

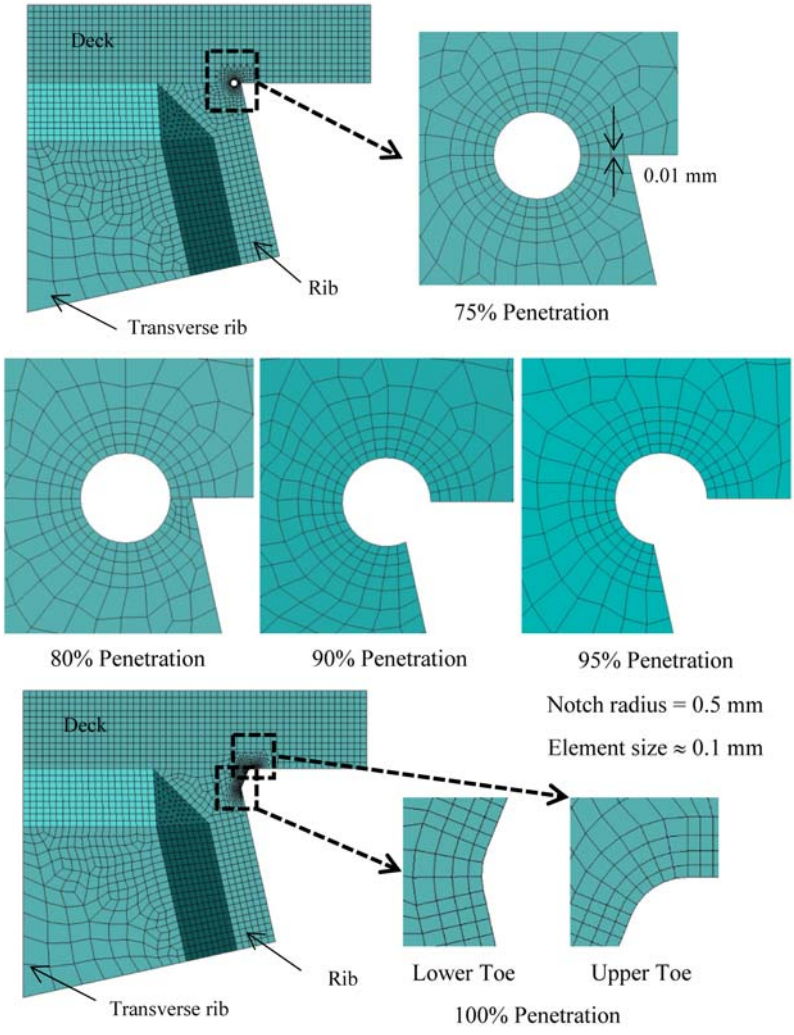

Figure 18. Detail of sub-models.

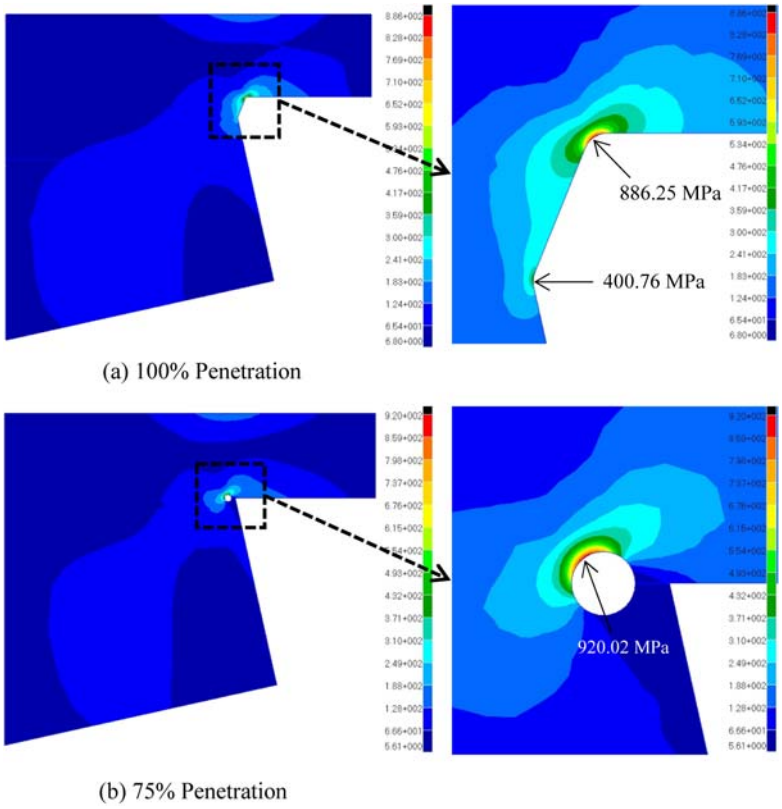

Figure 19. Effective notch stresses at the weld toes of the 100% penetration and weld root of the 75% penetration.

The loading condition in the global model represents the maximum load of 55 kN applied on the loading grip centered on top of the deck above the rib during the experiment. The two loading pads were also modeled. The rib-to-deck, rib-to-girder and girder-to-deck welds were all modeled explicitly in the global model. The weld size used in the global model and the subsequent sub-model was determined from the actual measurement of the tested specimens. However, no root gap was created in the global model for the 75% penetration specimens. Finite element analysis of both the global model and the sub-model was done using the commercial finite element software ABAQUS. To validate whether the global model is appropriate in simulation of local behavior around the weld toe and root, comparisons were made between the strain values obtained by FE analysis at 5 mm from the weld toe or the edge of the rib plate and those recorded at the same locations in the initial static test prior to the fatigue testing (Fig. 17). The agreement between the results of FE analysis and testing indicated that the local structural behavior at the proximity of the weld toe and root could be properly simulated.

Sub-models using 3D solid elements (HEX8) and elastic material properties similar to those used in the global model were created to evaluate the effective notch stresses at the weld toe and weld root. Nodal displacements were interpolated on the cut boundaries of the global model to generate loading for the sub-model. The details of the

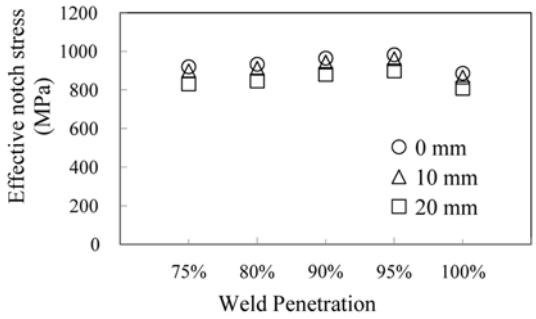

Figure 20. Variation of effective notch stress for different penetrations. Effective notch stress was evaluated at 0, 10, and 20 mm from the midpoint of the weld line.

sub-models are shown in Fig. 18. A notch radius of 0.5 mm was assumed such that the round notch of the 75% and 80% penetration can be contained in the rib-to-deck joint. Furthermore, the actual dimension of the 100% penetration weld bead inside the rib is smaller than that of the conventional weld (e.g., the weld bead outside the rib). Schijve (2012) suggested the adoption of a ratio of two dimensions, the radius and the height of the weld bead in consideration of a notch radius choice. In addition, to make the results comparable to that obtained in literature the notch radius size is chosen similar to that reported in (Miki, 2006) (Sim *et al*., 2012) who also employed the effect notch stress method. The size of elements located

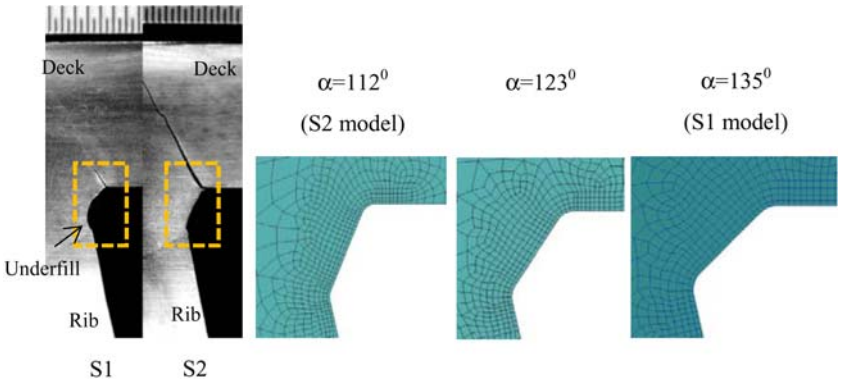

Figure 21. Typical weld configuration (left) and model of the 100% penetration with different open angles (right).

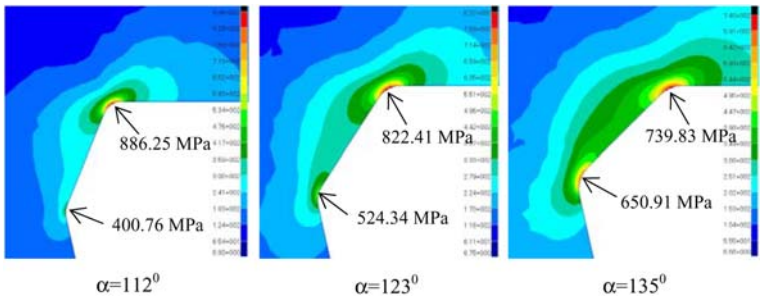

Figure 22. Distribution of effective notch stress at the upper and lower weld toes with different open angles.

along the curve of the radius was chosen as 0.1 mm according to recommendations in (Hobbacher, 2009) (Fig. 18). A root gap of 0.01 mm between the rib and deck plate was also assumed. Partial penetration including 75, 80, 90, and 95% penetration ratios were modeled in such a way that the tip of the effective notch radius matched the actual weld root.

Fig. 19 shows the contours of von Mises stress, which were used to evaluate the effective notch stresses at the weld toe and root. A comparison of the stresses at the upper and lower weld toes shows that under the given loading condition, the stress at the lower toe is about half that of the upper toe, indicating it is less likely for fatigue cracks to initiate at the lower toe. In fatigue testing, no cracks initiating at lower toes and propagating into the rib plate were identified. Instead, all cracks initiated from the upper toe and propagated upwards through the thickness of the deck plate (Fig. 9). As shown in Fig. 19, the maximum stress occurred on the upper side of the notch at the weld root of the partial penetration, which indicates that fatigue cracks initiating at weld roots may propagate into the deck plate and not into the weld metal. In the fatigue test, all the fatigue cracks were found to penetrate into the deck plate (Fig. 9). For partial penetration, a deeper penetration appeared to result in a slightly higher effective notch stress at the weld root (Fig. 20). This finding is somewhat consistent with the tendency reported by Sim and Uang (2012) who studied three penetration ratios of 40, 60, and 80%. Although 100% penetration yielded a lower effective notch stress than that obtained in all the partial penetration ratios, the margin of difference between the proposed 100% penetration and the traditional 75% penetration is merely 3.8%.

4.3. Effect of open angle at weld toe

To further investigate the cause of the significantly lower fatigue strength of S2 compared to S1, rib-to-deck joints were cut and observed at three sections located at 0 mm, 10 mm and 20 mm from the midpoint of the weld line. The observation of the etched surfaces reveals that the open angle of the weld toe in S1 appeared to be larger than that of S2, which is due to the existence of underfill at the lower weld toe (Fig. 21). Therefore, the effect of the open angle at weld toe was investigated. Three open angle values of 112^0, 123^0, and 135^0 were chosen to cover the range of the measured open angle at the weld toe in S1 and S2 (Fig. 21). It should be noted that an open angle of 112^0 was used in the sub-model of the 100% specimen illustrated in section 4.2, with corresponding FE analysis result shown in Fig. 19. The location of the upper weld toe was kept constant in all three cases of open angles, and the location of the lower weld toe was shifted on the edge of the rib plate to create the different upper toe open angles. The sub-modeling technique using the same element type and size at the weld toe, described in the preceding section 4.2, was used for the three cases.

The analysis results show the effect of the open angle on the effective notch stress at the upper weld toe (Fig. 22

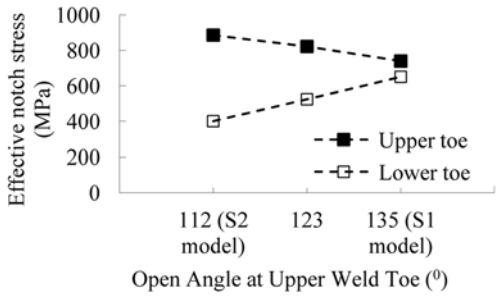

Figure 23. Effect of the open angle on the effective notch stress at the weld toe of the 100% penetration.

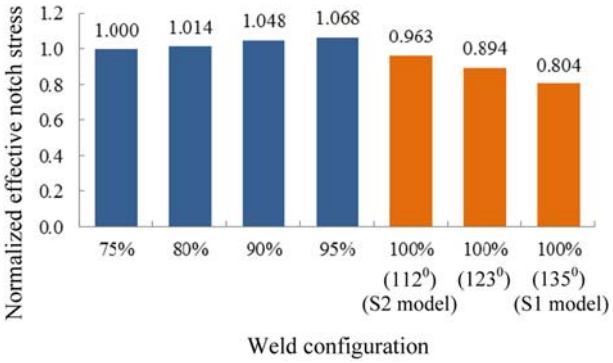

Figure 24. Variation of effective notch stress at weld root (for partial penetration) and weld toe (for 100% penetration with different open angles). Effective notch stress is normalized to that of 75% penetration.

& 23). A greater open angle at the upper weld toe appeared to result in a lower effective notch stress at the upper weld toe, but a higher stress at the lower weld toe. A decrease of 16.5% in stress was observed as the open angle increased from 112^0, which represents the weld toe configuration of S2, to 135^0, representing S1.

The results of normalized stress (Fig. 24) provide an insight into the fatigue test results. The stress at the weld root of S3 and S4 (i.e., partial penetration specimens) is higher than that at the weld toe of S1 and S2 (i.e., 100% penetration specimen). Furthermore, the stress appeared to decrease by about 19.6% for 100% ($\alpha=135^0$) compared to 75% penetration. A wider open angle which leads to a lower stress at the upper weld toe in S1 results in the superior fatigue strength of S1 compared to that of the remaining specimens (Fig. 8). The existence of cold lap and a narrower open angle at the weld toe of S2 may have made the fatigue strength of S2 approximately equal to that of the 75% penetration specimens (i.e. S3 and S4). The open angle of 135^0 may be a recommendation for further improving the proposed 100% weld configuration. The difference in stress between the upper and lower weld toes in the case of 135^0 is 13.7%. If the open angle is increased further, there may be a possibility of fatigue crack initiating at the lower weld toe.

5. Conclusions

The effectiveness of increasing weld penetration to improve the fatigue resistance of rib-to-deck welded joints was evaluated by fatigue tests on orthotropic deck specimens fabricated with 75% and proposed 100% penetration. Under the described loading conditions, cracks initiated from the weld toe inside the rib in specimens with 100% penetration, but the weld root for 75% penetration specimens. Cold lap may have been one of the major causes of the deteriorated fatigue resistance of one of the 100% penetration specimens. However, this detrimental effect of cold lap could possibly be avoided if the welding operation is improved. FEM analysis results indicated that a deeper partial penetration ratio results in a slightly higher effective notch stress. The effective notch stress at the crack initiation location in the 100% penetration specimens is lower than that obtained in the partial penetration specimens. In addition, the open angle appeared to have a significant effect on the effective notch stress at the weld toes of the 100% penetration specimens. An open angle of 135^0 at the upper weld toe is a possible recommendation to further improve the proposed 100% weld configuration. In conclusion, the proposed 100% penetration may enhance the fatigue resistance of rib-to-deck welded joints.

References

AASHTO (2010). *LRFD bridge design specifications. 5th edition,* AASHTO, Washington, DC.

Bocchieri, W. J. and Fisher, J. W. (1998). "Williamsburg Bridge replacement orthotropic deck as-built fatigue test." *ATLLSS Rep. No. 98-04*, Lehigh University, Bethlehem, PA.

Heiskanen, M. (2008). "A parametric fracture mechanics study of the effect of a cold lap defect on fatigue strength." *Journal of Structural Mechanics*, 41(3), pp. 119-136.

Hobbacher, A. (2009). *IIW Recommendations for fatigue design of welded joints and components*. WRC Bulletin 520, The Welding Research Council, New York.

JRA (2002). *Fatigue design guidelines for steel highway bridges.* Japan Road Association, Tokyo, Japan.

Mori, T. (2003). "Influence of weld penetration of fatigue strength of single-sided fillet welded joints." *Journal of Construction Steel of JSSC*, 10(40), pp. 9-15 (in Japanese).

Miki, C. (2006). "Fatigue damage in orthotropic steel bridge decks and retrofit works." *International Journal of Steel Structures*, 6(4), pp. 255-267.

Nishida, N., Sakano, M., Tabata, A., Sugiyama, Y., Okumura, M., and Natsuaki, Y. (2013). "Fatigue behavior of orthotropic steel deck with both side fillet welds between deck and trough ribs." *Proc. 68th JSCE Annual Meeting*, pp. I-572 (in Japanese).

Radaj, D. (1996). "Review of strength assessment of nonwelded and welded structures based on local

parameters." *International Journal of Fatigue*, 18, pp. 153-170.

Schijve, J. (2012). "Fatigue prediction of welded joints and the effective notch stress concepts." *International Journal of Fatigue*, 45, pp. 31-38.

Sim, H. B., Uang, C. M., and Sikorsky, C. (2009). "Effect of fabrication procedures on fatigue resistance of welded joints in steel orthotropic decks." *Journal of Bridge Engineering*, 14(5), pp. 366-373.

Sim, H. B. and Uang, C. M. (2012). "Stress analyses and parametric study on full-scale fatigue tests of rib-to-deck welded joints in steel orthotropic decks." *Journal of Bridge Engineering*, 17(5), pp. 765-733.

Kusumoto, T., Sakano, M., Tabata, A., Sugiyama, Y., Maeda, T., Arimochi, K., and Honda, N. (2012). "Influence of penetration depth in the longitudinal weld between deck and trough ribs on fatigue behavior of orthotropic steel deck." *Proc. 67th JSCE Annual Meeting*, pp. I-297 (in Japanese).

FHWA (2012). Manual for design, construction, and maintenance of orthotropic steel deck bridges. *Publication No. FHWA-IF-12-027*, US Department of Transportation, Federal Highway Administration.

Ya, S., Yamada, K., and Ishikawa, T. (2011). "Fatigue evaluation of rib-to-deck welded joints of orthotropic steel bridge deck." *Journal of Bridge Engineering*, ASCE, 16(4), pp. 492-499.